Solution Structure of the Immunodominant Domain of Protective Antigen GNA1870 of *Neisseria meningitidis**[*]

Francesca Cantini[‡], **Silvana Savino**[§], **Maria Scarselli**[§], **Vega Masignani**[§], **Mariagrazia Pizza**[§], **Giacomo Romagnoli**[§], **Erwin Swennen**[§], **Daniele Veggi**[§], **Lucia Banci**[‡], and **Rino Rappuoli**[§1]

From the [‡]*Centro Risonanze Magnetiche (CERM), University of Florence, Via L. Sacconi 6, 50019 Sesto Fiorentino, Italy and* [§]*CHIRON Vaccines Research Center, Via Fiorentina, 1, 53100 Siena, Italy*

GNA1870, a 28-kDa surface-exposed lipoprotein of *Neisseria meningitidis* recently discovered by reverse vaccinology, is one of the most potent antigens of *Meningococcus* and a promising candidate for a universal vaccine against a devastating disease. Previous studies of epitope mapping and genetic characterization identified residues critical for bactericidal response within the C-terminal domain of the molecule. To elucidate the conformation of protective epitopes, we used NMR spectroscopy to obtain the solution structure of the immunodominant 18-kDa C-terminal portion of GNA1870. The structure consists of an eight-stranded antiparallel β-barrel overlaid by a short α-helix with an unstructured N-terminal end. Residues previously shown to be important for antibody recognition were mapped on loops facing the same ridge of the molecule. The sequence similarity of GNA1870 with members of the bacterial transferrin receptor family allows one to predict the folding of this class of well known bacterial antigens, providing the basis for the rational engineering of high affinity B cell epitopes.

Neisseria meningitidis is a human pathogen implicated with sepsis and meningitis in children and young adults. Based on the immunological characteristics of the capsular polysaccharides, *N. meningitidis* strains are divided into 12 serogroups (1). Capsular polysaccharide-based vaccines have been produced for four of the five major meningococcal serogroups associated with invasive disease (A, C, Y, and W135) (2–4). Unfortunately, the capsular polysaccharide of serogroup B is poorly immunogenic, making this type of vaccine ineffective. Alternative strategies pointed toward the use of outer membrane proteins as targets for vaccine development. However, because of the antigenic heterogeneity of these proteins or phase-variable expression of their genes, they were unable to provide protection against a wide panel of serogroup B strains (5–10).

Three-dimensional structures of two neisserial antigens, NspA (11) and OpcA (12), have been solved, both showing a very similar architecture. They are outer membrane proteins constituted by a variable number of antiparallel β-strands connected by periplasm-faced and surface-exposed mobile loops that bear the epitopes responsible for bactericidal activity. Unfortunately, the external loops correspond to the highly vari-

able domains of the proteins, and therefore these antigens cannot be used to generate full protection over a population of different strains.

As an alternative strategy, reverse vaccinology was exploited for the identification of novel surface-exposed protein antigens to be used in a vaccine formulation against *Meningococcus* B. By this approach, several potential vaccine candidates were recognized, some of which are presently undergoing clinical trials.

Among them, genome-derived *Neisseria* antigen 1870 (GNA1870)[2] is a lipoprotein of unknown function that shares a weak sequence similarity to the B component of transferrin receptor produced by the pathogenic bacteria of *Neisseriaceae* and *Pasteurellaceae* (13). Bacterial transferrin receptor consists of two surface proteins, transferrin-binding proteins A and B (TbpA and TbpB), where TbpA is an integral transmembrane protein that probably serves as a channel for iron influx, whereas TbpB is an outer membrane lipoprotein that recognizes the host receptor Tf and binds iron (14). In addition to its crucial role in pathogenesis, TbpB of *N. meningitidis* (15, 16), *Haemophilus influenzae* (17), and *Moraxella catarrhalis* (18) have also been shown to elicit a strong bactericidal response and represent well studied vaccine candidates. *In vitro* and *in vivo* assays showed that GNA1870 is expressed on the surface of *Meningococcus*, is able to elicit good levels of antibodies with bactericidal activity, and induces passive protection in the infant rat model. Sequencing of the gene in a large panel of isolates showed that three variants of the protein can be distinguished, with levels of sequence similarity ranging from 62.8% between variants 1 and 3 to 74.1% between variants 1 and 2 and 84.7% between variants 2 and 3. Although the three alleles display very low levels of cross-bactericidal response, a vaccine containing representative molecules of the three variants of GNA1870 may be able to protect against all *N. meningitidis* strains (13).

To dissect the nature and architecture of protective epitopes of GNA1870, we performed an epitope mapping by reproducing the GNA1870 sequence with overlapping synthetic peptides. On the basis of the resulting antigenic profile, GNA1870 has been subdivided into three regions encompassing amino acids 8–100 (region A), 101–164 (region B), and 165–255 (region C) of the mature protein. A bactericidal monoclonal antibody (mAb502) was found to recognize a conformational epitope within the whole BC region, and arginine 204 was found to be absolutely required for the binding (19). Furthermore, independent studies have identified the sequence Glu[146]-Arg[149] as part of a bactericidal epitope (20).

Here we present the solution structure of the BC region of variant 1 antigen GNA1870 obtained by NMR spectroscopy and a map of residues essential for antibody recognition. The protein adopts an eight-

stranded β-barrel conformation, which encompasses amino acids 151–255, whereas the remaining residues include a short α-helix (138–141) and a flexible tail (101–137), which probably serves as a linker to the N-terminal A region of the protein. This is the first structure of a protective antigen of *N. meningitidis* identified by reverse vaccinology. Mapping of bactericidal epitopes on the solved structure of GNA1870 will help to envisage the mechanism of immune recognition and to design novel vaccine candidates.

Furthermore, the position of these epitopes on the global architecture of the BC domain can give a better perspective on the overall organization of immunogenic domains as well as define a possible area more directly involved in contacting the binding site of the antibody.

MATERIALS AND METHODS

Protein Expression and Fermentation—The *Gna1870-BC* gene fragment was amplified by PCR on the chromosomal DNA of the *N. meningitidis* MC58 strain and cloned into pET21b$^+$ vector (Novagen) under the control of the T7 promoter. The protein was expressed in the *Escherichia coli* BL21 (DE3) strain as a C-terminal histidine fusion. As a result of the cloning sites, three amino acids have been added to the protein, namely a Met at the N terminus and a Leu-Glu at the C terminus prior to the six histidines.

E. coli BL21(DE3) (pET21b-GNA1870-BC) was grown on M9 minimal medium with the addition of vitamin solution (1 mg/liter thiamine, 1 mg/liter biotin, 1 mg/liter piridoxin HCl, 1 mg/liter niacinamide) and ampicillin (0.100 g/liter), containing glucose and NH$_4$Cl as the sole carbon and nitrogen source, respectively. Temperature was maintained at 37 °C, and the pH was controlled at 7.2 by the addition of NaOH (4 M). For isotope monolabeling, an overnight culture of the expression host was inoculated in a 2-liter bioreactor system (Applikon) and grown on 1 liter of minimal medium containing 3.0 g of ^{15}NH$_4$Cl (98% isotopic enrichment, Aldrich) and 6.0 g of glucose or containing for the bilabeling 3.0 g of ^{15}NH$_4$Cl (98% isotopic enrichment, Aldrich), 2.5 g of glucose, and a starvation-controlled exponential glucose feed of 4.5 g (^{13}C$_{1-6}$, 99% isotopic enrichment, Sigma) after depletion of initial glucose (visualized by increase in optical density value). The culture was induced after growth for one duplication time in the presence of labeled nutrients at A_{590} of 4.0 with 1.4 mM sterile filtered isopropyl 1-thio-β-D-galactopyranoside (Sigma) for 70 min. The cells were harvested by centrifugation (8000 × *g* for 30 min), and the cell paste was stored at −80 °C. A yield of 11.5 g of wet cell paste was obtained from 1 liter of culture medium (final A_{590} = 6.2).

Purification and Sample Preparation of GNA1870-BC—Isopropyl 1-thio-β-D-galactopyranoside-induced cells expressing the recombinant ^{15}N- and ^{13}C-labeled GNA1870-BC were resuspended in 50 mM phosphate buffer, pH 8.0, containing 300 mM NaCl and French-pressed. By centrifugation at 39200 × *g* for 45 min, the soluble fraction was separated from the inclusion bodies. The supernatant enriched by the GNA1870-BC protein was loaded on a metal chelate affinity chromatography column. A fast protein liquid chromatography system (Amersham Biosciences) has been used.

After the flow-through recovery, the column was extensively washed with the same buffer used for the pellet resuspension, an additional wash was done with 50 mM phosphate buffer, pH 8.0, containing 300 mM NaCl and 55 mM imidazole. The protein was finally eluted in 50 mM phosphate buffer, pH 8.0, containing 300 mM NaCl and 125 mM imidazole. The partially purified GNA1870-BC was dialyzed against 50 mM sodium acetate buffer, pH 5.5.

To reach a higher purity level, another purification step was done, and the protein was further purified using a 0–1 M NaCl gradient in 50 mM
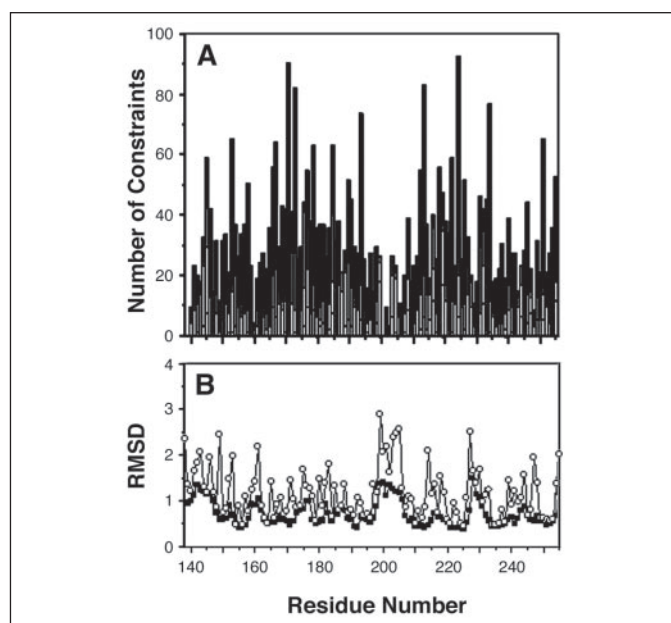

FIGURE 1. **Number of meaningful NOEs and RMSD values per residue of the region 139–255 of GNA1870-BC.** *A*, *white*, *light gray*, *dark gray*, and *black bars* indicate intra-residue, sequential, medium-range, and long-range connectivities, respectively. *B*, RMSD values per residue to the mean structure for the backbone (*filled squares*) and all heavy atoms (*open circles*) of the REM family of 30 conformers.

sodium acetate buffer, pH 5.5, on a SP-Sepharose Fast Flow column (Amersham Biosciences). The purest fractions were pooled and concentrated to 2 mM using a vacuum concentrator system (CentriVap-Labconco). Purified GNA1870-BC was then dialyzed against 20 mM phosphate buffer, pH 7.0, and the final concentration used for NMR characterization was 1.0 mM.

NMR Structural and Dynamic Characterization of GNA1870-BC—The NMR spectra were acquired at 298 K on Avance 800 and 600 Bruker spectrometers, the former equipped with a triple resonance cryoprobe. The NMR experiments, used for the backbone and the aliphatic side-chain resonance assignments recorded on ^{13}C/^{15}N- and ^{15}N-enriched and unlabeled GNA1870-BC samples, are summarized in supplemental Table S1. The ^{1}H, ^{13}C, and ^{15}N resonance assignments of GNA1870-BC are reported in supplemental Table S2. Some amide resonances are missing for residues belonging to the N and C termini segments. Overall, the resonances of 95% of the carbon atoms, 97% of the nitrogen atoms, and 90% of the protons (calculated considering the segment 103–255) were assigned. ^{3}JHNHα coupling constants, determined through the *HNHα* experiment, were transformed into backbone dihedral φ angles through the Karplus equation (21). Backbone dihedral ψ angles for residues (i-1) were also determined from the ratio of the intensities of the $d_{\alpha N}(i-1,i)$ and $d_{\alpha N}(i,i)$ NOEs obtained from the ^{15}N-edited NOESY-HSQC spectrum (22). Distance constraints for structure determination were obtained from ^{15}N- and ^{13}C-edited three-dimensional NOESY-HSQC experiments acquired with a mixing time value of 80 ms for both experiments.

2242 meaningful proton-proton distance restraints (Fig. 1*A*) of 3340, together with 74 φ and 80 ψ backbone dihedral angle restraints, were included in the structure calculations. Distance restraints are considered meaningless and not used in the calculation when they would be satisfied in all possible conformations or are between two hydrogen atoms at fixed distances (*i.e.* constraints between geminal hydrogen atoms).

Residual dipolar couplings have been measured in the presence of an external orienting medium constituted by a binary mixture of C12E5

(pentaethylene glycol dodecyl ether, >98% of purity, Fluka) and neat *n*-hexanol (>99% of purity, Fluka), which form a stable liquid crystalline phase made of neutral aggregates (called bicelles) in the temperature range from 298 to 312 K (23). The molar ratio of C12E5 to *n*-hexanol was 0.96, and the C12E5/water ratio was 5% w/w. One-bond ^{1}H-^{15}N coupling constants were measured at 298 K and 800 MHz using the in-phase/anti-phase method (24). A total of 114 residual dipolar coupling values have been measured from amide signals not overlapped in the HSQC spectrum, and they ranged from −10 to +14 Hz. Of them, 85 RDC values derived from residues not experiencing R_1 and/or R_2 values outside the average values were used for structure calculations.

Structure calculations were performed using the program CYANA (25). The CANDID module of CYANA (25) was used for automated assignment of the NOESY cross-peaks, followed by a manual check prior to the final calculations. 400 random conformers were annealed in 10,000 steps. The RDC values were included in the last steps of structure calculations, and the χ tensor parameters, obtained with FANTAORI-ENT, were optimized through iterative cycles of PARAMAGNETIC-DYANA (www.postgenomicnmr.net) until convergence (26).

The family of the best 30 structures in terms of target function was then subjected to restrained energy minimization with the AMBER 5.0 package (27). The NOE and torsion angle constraints were applied with force constants of 50 kcal mol^{-1}Å^{-2} and 32 kcal mol^{-1} rad^{-2}, respectively. The quality of the structures was evaluated using the program PROCHECK-NMR (28).

RMSD values per residue of the restrained energy minimization family of 30 conformers, which were best fitted over the segment 139–255 and have been calculated with respect to the mean structure for the backbone and for heavy atoms (Fig. 1). The conformational and energetic analysis of the final REM family of GNA1870-BC is reported in supplemental Table S3.

^{15}N-R_1, -R_2, and steady-state heteronuclear NOEs, which can provide information on internal mobility as well as on the overall protein tumbling rate, were measured with pulse sequences as described by Farrow *et al.* (29). R_2 was measured using a refocusing time of 450 μs. In all experiments, the water signal was suppressed with a "water flip-back" scheme (30). Average R_1, R_2 and ^{1}H-^{15}N NOE values of 1.38 ± 0.04 s^{-1}, 14.8 ± 0.2 s^{-1}, and 0.70 ± 0.03 are found, respectively, at 600 MHz. The experimental relaxation rates were used to map the spectral density function values, $J(\omega_H)$, $J(\omega_N)$, and $J(0)$ using the following expressions (31),

$$J_{eff}(0) = \frac{\left[6R_2 - 3R_1 - \frac{18}{5}R_1(NOE - 1)\frac{\gamma_N}{\gamma_H} \right]}{(3d^2 + 4c^2)} \quad \text{(Eq. 1)}$$

$$J(\omega_N) = \frac{4R_1}{(3d^2 + 4c^2)} \left[1 - \frac{7}{5}(NOE - 1)\frac{\gamma_N}{\gamma_H} \right] \quad \text{(Eq. 2)}$$

$$J(\omega_H) = 0.2 R_1(NOE - 1)\frac{4}{d^2}\frac{\gamma_N}{\gamma_H} \quad \text{(Eq. 3)}$$

where $d = (\mu 0 h \gamma_H \gamma_N / 8\pi^2 r_{NH}{}^3)$ and $c = \omega_N(\sigma - \sigma_\perp)/\sqrt{3}$.

Molecular Modeling—Homology models for GNA1870-BC variants 2 and 3 were obtained with the MODELLER 6 version 2 software (32) using the average NMR structure of GNA1870-BC variant 1 as a template.

The same software has been used to model the C-terminal lobe of *N. meningitidis* TbpB onto the atomic coordinates of GNA1870-BC. The raw structure models have been refined by energy minimization using AMBER 5.0 and their geometries checked with PROCHECK.
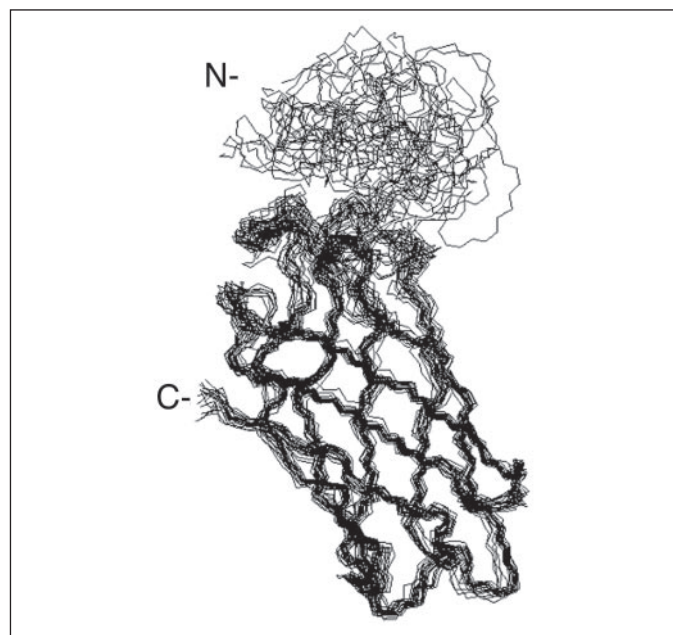

FIGURE 2. **Solution structure of GNA1870-BC.** Backbone traces for the twenty lowest energy conformers are superimposed. The β-barrel backbone (residues 151–255) exhibits RMSD values to the mean structure of 0.78 Å. In contrast, residues 115–150 display large motional freedom. The N and C termini are indicated.

RESULTS

Structure and Dynamics of GNA1870-BC—Antigen GNA1870 is a surface-exposed lipoprotein of 255 residues with a signal peptide of 19 amino acids and a predicted molecular mass of 28,000 Da. Conformational protective epitopes have been previously mapped onto the C-terminal BC region (residues 101–255) of the molecule (19, 20). To further investigate the immunogenic features of GNA1870 and to determine the solution structure of its protective moiety, we expressed the BC domain (amino acids 101–255) of the MC58 allele (variant 1) in *E. coli*.

Analytical gel filtration analysis showed that GNA1870-BC was eluted in fractions corresponding to a monomeric state for the protein. The electrospray ionization-mass spectrum indicated a mass of 17,595 Da, which corresponds to the cloned construct. The far-UV CD spectrum of GNA1870-BC had features characteristic of a folded protein with a large amount of β-sheet. The characteristic minimum of a random coil protein at 198 nm is not present in the spectrum. The ^{1}H-^{15}N HSQC spectra of GNA1870-BC show well dispersed resonances indicative of an essentially folded protein (supplemental Fig. S1).

Heteronuclear relaxation rates, whose values are affected by the dynamic properties of the molecule, were essentially homogeneous along the entire polypeptide sequence, with the exception of residues located at the C and N termini (supplemental Fig. S2). The correlation time for the molecule tumbling (τ_m), as estimated from the R_2/R_1 ratio, is 10.0 ± 1.0 ns, as expected for a protein of this size in a monomeric state (8, 9), thus confirming the gel filtration analysis. From the spectral density function analysis (supplemental Fig. S2), it appears that the residues in the 101–151 region have $J(\omega_H)$ values higher than average, consistent with significantly lower heteronuclear NOE values and particularly with the lack of long range proton-proton NOEs. This behavior is the consequence of local motions in the ns–ps time scale, *i.e.* faster than the overall protein tumbling rate for the N terminus segment.

The solution structure of GNA1870-BC, based on distance, angle, and residual dipolar coupling (supplemental Fig. S3) constraints, consists of an eight-stranded antiparallel β-barrel (151–255) surmounted by the short α-helix α1 (138–141). The rest of the molecule (101–137) is characterized
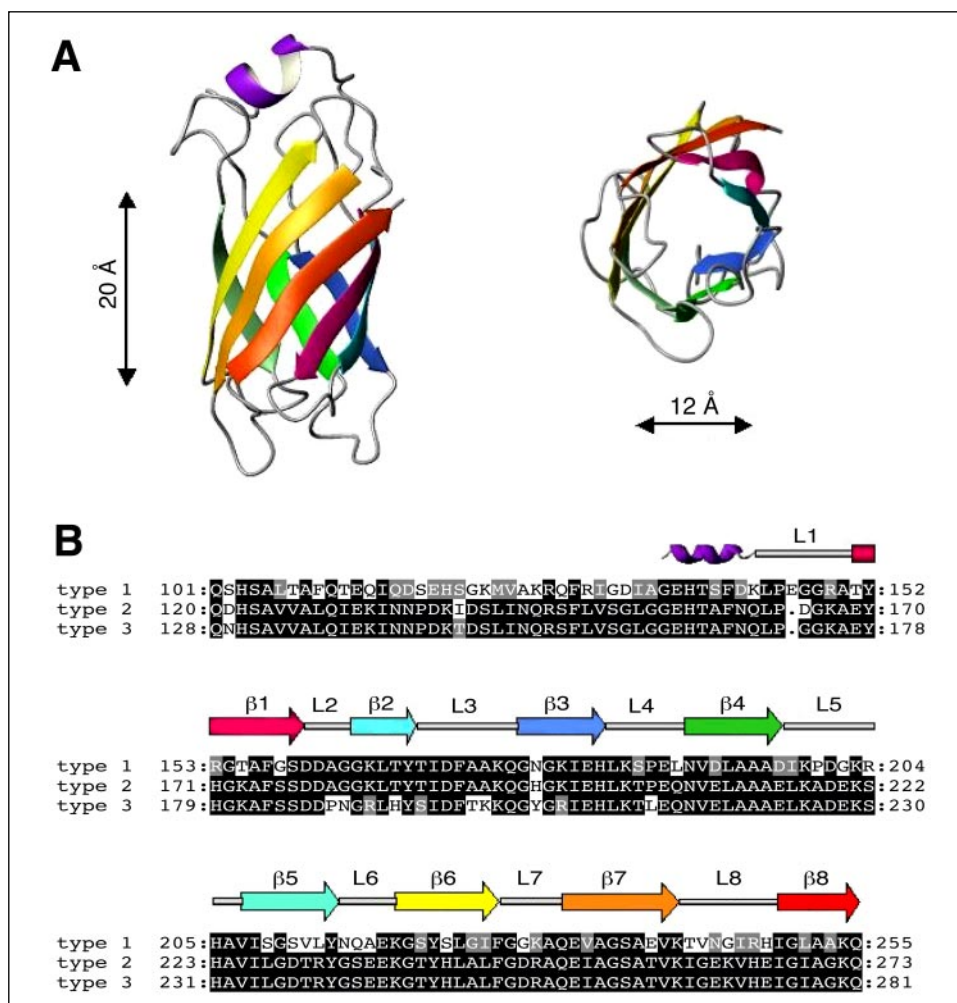
FIGURE 3. **The molecular architecture of GNA1870-BC.** *A*, ribbon diagram of side and top view of the GNA1870-BC domain. Residues 115–143 are omitted for clarity in the *top view*. *B*, sequence alignment of the prototypic members of the three GNA1870 variants. Identical residues are *white* on *black background*, whereas conservative substitutions are in *gray*. The distribution of secondary structure elements is reported *above* the sequences. α_1 helix and β-strands are depicted as *coil* and *arrows*, respectively.

by a low number of long range NOEs, which determine higher RMSD values (Fig. 2). This is in accordance with the structure prediction (bip.weizmann.ac.il/fldbin/findex), which indicated that the segment 101–137 is the longest disordered region for this construct. In contrast, the β-barrel domain is well defined, with only one loop showing some level of conformational variability (Fig. 1).

The GNA1870-BC β-barrel had a height of 20 Å and a main chain diameter of ~12 Å (Fig. 3A), which was stabilized by a strong hydrogen bond network linking all of the β-strands. The core was characterized by several hydrophobic interactions, which involve buried aromatic and aliphatic residues (Leu[166] (β2), Ile[181] (β3), Val[191] (β4), Leu[193] (β4), Ile[208] (β5), Val[212] (β5), Tyr[222] (β6), Val[234] (β7), Val[240] (β7), Ile[249] (β8), and Leu[251] (β8)). Other hydrophobic residues localized within the cavity are Ile[170], Leu[184], and Ile[198].

Sequence alignment of the three representative alleles shows that, as opposed to integral outer membrane proteins, regions of extensive variability of GNA1870 are not associated with mobile loops but instead are spread on the whole molecule, suggesting that the entire protein is exposed to immune recognition (Fig. 3B).

In an attempt to obtain some indication about the putative biological function of GNA1870, we performed a search for structurally related proteins in the Protein Data Bank (PDB) using the DALI (33), SCOP, and CATH (34) routines. By this screening, we identified domain 2 of the α-subunit of the quinohemoprotein amine dehydrogenase from *Paracoccus denitrificans* (PDB code 1JJU) (35) and the outer membrane protein NspA from *N. meningitidis* (PDB code 1P4T) (11) as the closest

structural homologues. Both structural neighbors adopt an antiparallel eight-stranded β-barrel fold. However, although the first is a cytoplasmic enzyme catalyzing the oxidation of biological amines (36), NspA is an integral outer membrane protein sharing homology to members of the opacity (Opa) family proteins, which are involved in adhesion to host cells (37). Other structural homologues include proteins and protein domains from a variety of prokaryotic and eukaryotic organisms playing different biological roles (data not shown), thus indicating that this architecture is not suggestive of any specific function.

Calculation of the molecular surface of GNA1870-BC showed the presence of an extensive hydrophobic region on one side of the β-barrel (Fig. 4A), which contained strands β1, β6, β7, and β8, whereas charged residues were mostly located on loop regions at the two extremes of the barrel. On the other face of the molecule, a well defined negative patch is present together with scattered positive charges.

Structural models of each of the other two variants, calculated using the structure here determined as the template, showed that variants 2 and 3 have very similar electrostatic potential surfaces (Fig. 4, B and C). The presence of a conserved hydrophobic patch on one side of the three variants of GNA1870-BC, whereas other sides are characterized by a scattered positive and negative charges, suggests that this region might have a functional role.

Epitope Mapping—Recent studies have mapped two possible bactericidal epitopes on the BC region of GNA1870 variant 1 (19, 20). The first is located within the B region and corresponds to residues Glu[146]-Arg[149], which form the loop connecting α1 to the β-barrel (20). The
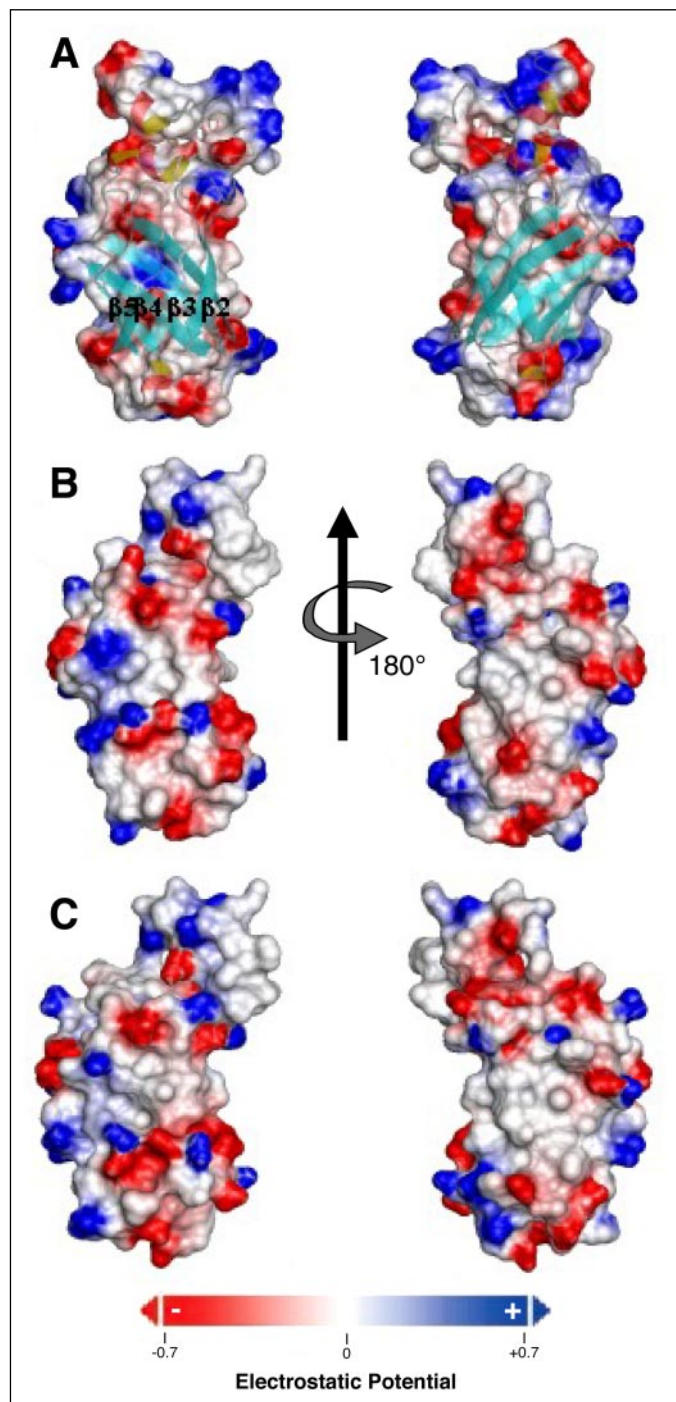
FIGURE 4. **Electrostatic surfaces of the three GNA1870 variants calculated with the MOLMOL program (44).** The molecular surface of the GNA1870-BC structure of variant 1 (MC58 strain (*A*) is compared with computer models of variant 2 (*B*) and variant 3 (*C*) type strains. The proteins are shown rotated by +180 and −180°, respectively. Areas of negative, positive, and neutral electrostatic potential are depicted in *red*, *blue*, and *white*, respectively. *Scale bar* is shown. The values of electrostatic potential are given in units of *e*/Å (*e* is electron charge). All of the surfaces present a conspicuous patch of exposed hydrophobic residues (*white*) along one side of the barrel (*right side*), whereas the opposite face presents a mostly polar character where positive (*blue*) and negative (*red*) charges are scattered.

second epitope maps within the C region on loop 4 of the barrel and contains the Arg[204], which is absolutely required for immune recognition by mAb502 (19). Both epitopes reside on structurally less well defined loops located on the same edge of the molecule, which may be flexible (Fig. 5*A*).
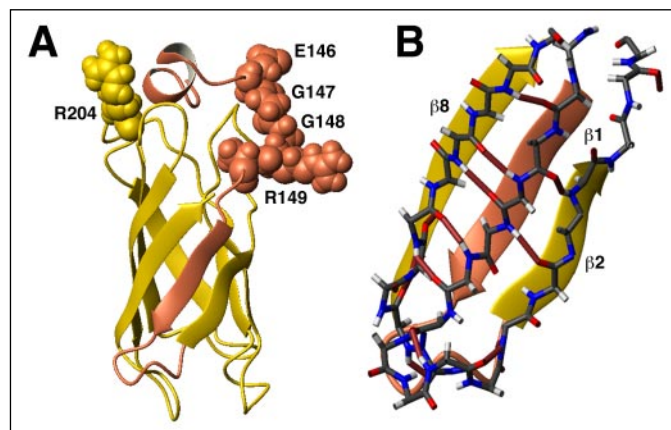

FIGURE 5. **Epitope mapping on GNA1870.** *A*, B and C subregions are colored onto the ribbon diagram in *coral* and *gold*, respectively. The tract corresponding to residues 115–137 is omitted for clarity. The amino acids involved in the formation of bactericidal epitopes are represented as *space fill* and labeled. *B*, magnified view of the connection between β1- and adjacent β2- and β8-strands. The hydrogen bond network, which provides the spatial proximity of B and C regions required for proper recognition of the bactericidal epitopes, is evidenced in *brown*. Hydrogen bonds were identified with the MOLMOL program (44); a hydrogen bond was assigned whenever donor and acceptor atoms were within 2.4 Å and the angle between the CO and NH vectors was smaller than 35°.

Our previous work has demonstrated that the integrity of the BC region is a necessary prerequisite to inducing a bactericidal response. Furthermore, when mixed together, separate B and C fragments were efficiently recognized in Western blot by the bactericidal antiserum, leading to the hypothesis that B and C are able to reconstitute *in vitro* the functional epitope (19). These results can be better interpreted with the availability of the structure of the BC fragment. The inspection of intramolecular connections shows that residues within β1 are engaged in a network of 4 and 5 hydrogen bonds, respectively, with β2 and β8 (Fig. 5*B*). The strength provided by this set of connections can possibly explain the propensity of B and C to tightly assemble and eventually reconstitute a stable structural unit, thus explaining previous *in vitro* results.

A Structure Common to Transferrin-binding Proteins—To shed light on the possible functional role of protein GNA1870, homology searches were performed using different algorithms and protein databases.

The results indicate that no significant similarity can be detected between the entire GNA1870 and proteins from any other microorganism deposited to GenBank[TM], thus suggesting the very high specificity of this protein for the genus *Neisseria*. The same result was obtained when the protein sequence was searched against the list of unfinished genome sequences (www.ncbi.nlm.nih.gov/blast/Blast.cgi), which enclose predicted open reading frames from 261 diverse bacterial species.

However, when searching only with the BC domain, a very low similarity (28% identity over 146 amino acids) was detected with the C-terminal portion of transferrin-binding proteins B from several bacterial species.

Previous studies identified seven short segments of sequence similarity between the N- and C-terminal halves of TbpBs, suggesting that the two domains might share similar three-dimensional folds (38, 39). Sequence similarity detected between GNA1870-BC and TbpBs involved six of the seven conserved boxes identified among TbpBs (Fig. 6), suggesting that these proteins might have structural or functional similarities.

A recent publication has identified by site-directed mutagenesis some residues of the meningococcal TbpB implicated in the recognition and
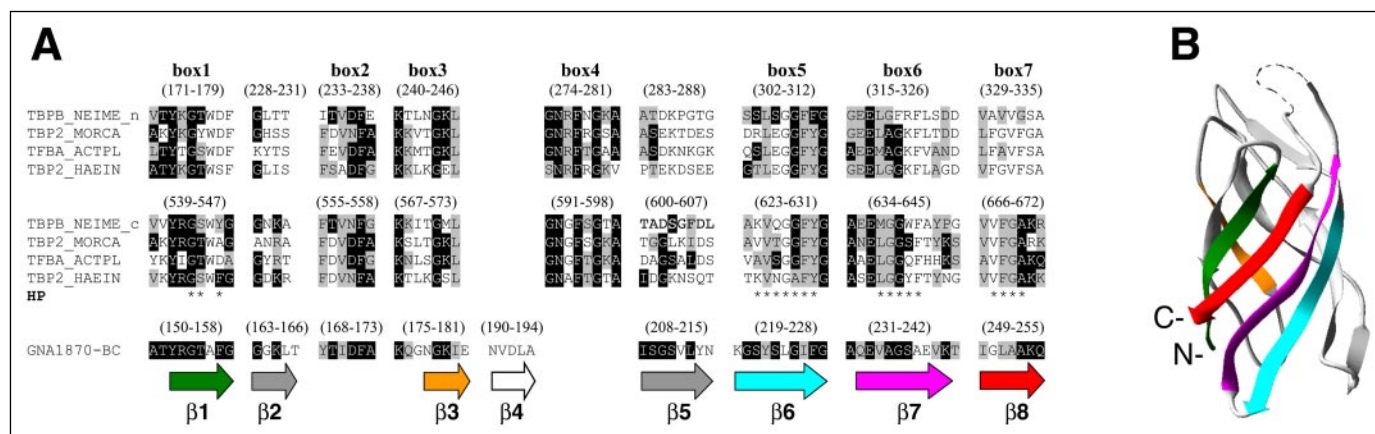
FIGURE 6. **Structural relationship between GNA1870-BC and TbpBs.** *A*, seven boxes of sequence conservation are identified superimposing the N- and C-terminal lobes of TbpBs from different pathogenic species (*NEIME*, *N. meningitidis*; *MORCA*, *M. catarrhalis*; *ACTPL*, *Actinobacillus pleuropneumoniae*; and *HAEIN*, *H. influenzae*). Reported amino acid segments are *numbered* according to the sequence of the *N. meningitidis* TbpB molecule. Positions identical between GNA1870-BC and at least one member of TbpBs are *white* on *black background*. Conservative substitutions are in *gray*. The arrows mark the position of GNA1870-BC β-strands, and *asterisks* label residues forming the conserved hydrophobic patch (*HP*). *B*, three-dimensional model of the C-terminal half of *N. meningitidis* TbpB obtained according to the alignment reported in *A*. Protein segments corresponding to β-strands matching the TbpB boxes are colored following the same scheme of *A*.

binding of human transferrin (40). All of these residues are located elsewhere with respect to the regions of similarity to GNA1870, thus indicating that the weak homology can only be predictive of a similar fold but not of a similar transferrin-binding activity. This observation was also confirmed by *in vitro* assays, which have definitely proved the inability of GNA1870 to bind transferrin (13). The segments of GNA1870 conserved with TbpBs boxes correspond nicely to β-strand units β1 (aligning with box 1), β3 (aligning with box 3), β6 (aligning with box 5), β7 (aligning with box 6), and β8 (aligning with box 7) (Fig. 6*A*). Conversely, box 2 corresponds to part of loop 2, and box 4, which is extremely well conserved among all TbpBs, does not have a match in the protein sequence of GNA1870. Secondary structure prediction analysis indicates a clear β-sheet propensity for both TbpB lobes (data not shown). This analysis supports the hypothesis that N- and C-terminal lobes of TbpBs have a domain architecture similar to the BC domain of GNA1870. A three-dimensional model constructed for the C-terminal portion of the *N. meningitidis* TbpB protein on the basis of the alignment presented in Fig. 6*A* confirms this possibility (Fig. 6*B*). However, the presence of a box conserved among TbpBs and missing from the protein sequence of the *Meningococcus* B antigen argue for some functional specificity of TbpBs, which is not shared with GNA1870.

Furthermore, four of the five β-strands (β1, β6, β7, and β8), corresponding to the conserved TbpB boxes, are also involved in the formation of the hydrophobic patch of the GNA1870 molecule, thus indicating that this feature is conserved among the two groups of proteins. This portion of the molecule could be involved in the interaction with specific molecular partners or as a domain-domain interface.

DISCUSSION

GNA1870 is a surface-exposed lipoprotein identified by genome analysis of the MC58 strain of *N. meningitidis*. This protein exists in three genetic variants displaying very low cross-reactivity. However a combination of the three variants could potentially cover the whole variability of *Neisseria* population (13). On the basis of our previous immunological studies, three regions, A, B, and C, were mapped within antigen GNA1870. Although linear epitopes were mostly contained within region A, the bactericidal response was directed against conformational epitopes formed by the combination of the B and C region and involving Arg[204] (19) and the Glu[146]-Arg[149] region (20).

In this study, we have determined the NMR solution structure of the

C-terminal antigenic domain of GNA1870 variant 1 as a first step to understanding the structure/immunogenicity relationship that makes a protein a potential vaccine candidate. Structural alignment revealed high similarity between the β-barrel of GNA1870-BC and the *N. meningitidis* NspA antigen. However, although NspA is totally embedded in the outer membrane, GNA1870 is fully surface-exposed, and therefore its structure is not affected by the membrane environment. Accordingly, GNA1870 displays a cavity filled with hydrophobic residues, as opposed to NspA and other canonical porins, where hydrophobic and aromatic side chains typically protrude outside of the barrel, establishing hydrophobic interactions with aliphatic chains of membrane phospholipids. Furthermore, unlike classical porins, where variability is mainly associated with exposed loops, the different topology of GNA1870 implies a different distribution of variable regions. Accordingly, the sequence variability observed among the three genetic variants, which usually reflects immunological pressure, shows a homogeneous distribution along the entire molecule and does not cluster within any restricted area.

The inspection of the electrostatic potential associated to BC domain surface reveals a compact hydrophobic patch formed by residues located within β-strands 1, 6, 7, and 8. These residues are not associated with extensive sequence variation among different alleles, and computer modeling of prototype variants 2 and 3 molecules confirm the presence of similar hydrophobic areas. Different scenarios can be envisaged to explain the presence of this patch: (i) this side of the molecule represents the site of contact with the outer membrane, (ii) it is involved in the interaction with other partner molecules, or (iii) it is juxtaposed onto the N-terminal domain of the molecule. In all cases, this face of the barrel is not likely to be directly exposed to immune recognition.

The availability of the BC structure can help to rationalize the importance of the integrity of this region for the induction of a bactericidal response. Arg[204], which plays a prominent role in inducing variant-specific bactericidal response, is located on the tip of loop 4. Therefore we could hypothesize that the entire conformational epitope is contained within the C region. However, the fact that B is necessary for the bactericidal activity indicates a direct role of this region either in providing additional residues to complete the conformational epitope or, alternatively, ensuring the structural integrity of the β-barrel. Fig. 5 shows that strand β1 of B forms a network of hydrogen bonds on both sides, respectively, with β2 and β8, acting as a molecular zipper able to
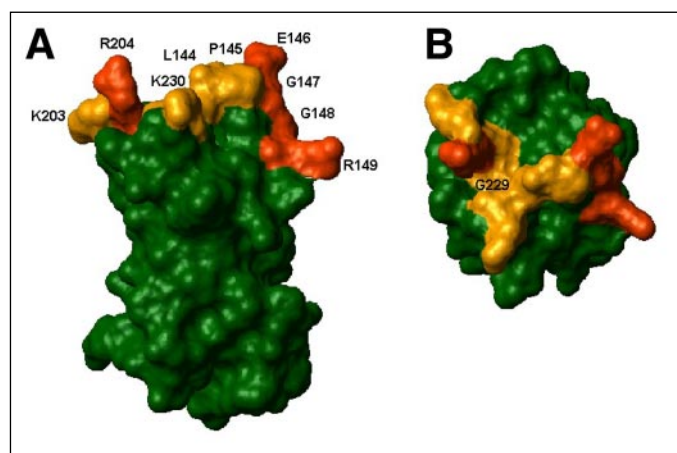
Solution Structure of Antigen GNA1870

FIGURE 7. **Molecular surface of GNA1870-BC.** Side (*A*) and top (*B*) view of the solvent-accessible area of GNA1870-BC has been calculated with MOLMOL software, using as a probe a sphere with a radius of 1.4 Å. Amino acids involved in the bactericidal epitope are *highlighted* in *dark orange*. Leu[144], Pro[145], Lys[203], Gly[229], and Lys[230], which have been included in the antigenic area, are colored in *pale orange*. Residues 101–143 are omitted for clarity.

close and hold tightly the β-barrel ring. The tendency of this conformation to properly fold could explain the finding that the conformational epitope can be reconstituted *in vitro* by the simple addition of domains B and C (19). Once formed, the resulting rigid architecture can provide a suitable scaffold to properly expose critical residues to the immune system.

Fig. 7 shows the reciprocal position of the residues so far identified as implicated in the bactericidal response (Glu[146], Gly[147], Gly[148], Arg[149], and Arg[204]). These residues define two regions that together with residues Leu[144], Pro[145], Lys[203], Gly[229], and Lys[230] could constitute the same epitope of GNA1870-BC.

The solvent-accessible area of such a putative epitope, calculated using a sphere of 1.4 Å of radius as a probe, corresponds to 1096 Å^2. This value is in the order of magnitude of the estimated area for single epitopes on the basis of crystallographic data (41–43).

Despite various attempts to functionally characterize protein GNA1870, its biological role still remains undefined. A weak amino acid sequence similarity detected between the BC domain and a family of transferrin-binding proteins of various organisms had initially directed functional studies toward this conclusion. However, all attempts to demonstrate a possible binding affinity of GNA1870 to human transferrin failed, thus suggesting that the observed homology was more indicative of a structural rather than of a functional similarity. TbpBs are characterized by a bi-lobed structure in which the N- and C-terminal lobes are each constituted by seven short sequence motifs well conserved between the two domains. These blocks would confer an overall conserved fold to the two distal portions of TbpBs. Alignment of GNA1870 with each of the two putative lobes of TbpBs showed that most of the previously recognized boxes correspond to β-strands forming the barrel. This result supports the idea that the two halves of TbpBs share a common fold, analogous to that determined for the C terminus of GNA1870. Furthermore, the hydrophobic patch is also conserved, suggesting a similar role for this region for TbpBs.

The NMR solution structure of GNA1870 therefore provided the opportunity to model TbpBs (Fig. 6*B*), thus giving further insight on the structure/function relationships of this important class of pathogenicity factors. Finally, given the marked immunogenic properties common to TbpBs and GNA1870, we can suggest a relevant role of this architecture in the mechanisms of epitope exposure to the immune system.

REFERENCES

1. Branham, S. E. (1953) *Bacteriol. Rev.* **17,** 175–188
2. Gotschlich, E. C., Liu, T. Y., and Artenstein, M. S. (1969) *J. Exp. Med.* **129,** 1349–1365
3. Vedros, N. A. (ed) (1987) *Evolution of Meningococcal Disease*, CRC Press, Inc., Boca Raton, FL
4. Frasch, C. E. (1989) *Clin. Microbiol. Rev.* **2,** (suppl.) S134–S138
5. Bjune, G., Hoiby, E. A., Gronnesby, J. K., Arnesen, O., Fredriksen, J. H., Lindbak, A.-K., Nokleby, H., Rosenqvist, E., Solberg, L. K., and Closs, O. (1991) *Lancet* **338,** 1093–1096
6. de Moraes, J. C., Perkins, B. A., Camargo, M. C., Hidalgo, N. T., Barbosa, H. A., Sacchi, C. T., Land Gral, I. M., Gattas, V. L., Vasconcelos, H., Plikaytis, B. D., Wenger, J. D., and Broome, C. V. (1992) *Lancet* **340,** 1074–1078
7. Perkins, B. A., Jonsdottir, K., Briem, H., Griffiths, E., Plikaytis, B. D., Hoiby, E. A., Rosenqvist, E., Holst, J., Nokleby, H., Sotolongo, F., Sierra, G., Campa, H. C., Carlone, G. M., Williams, D., Dykes, J., Kapczynski, D., Tikhomirov, E., Wenger, J. D., and Broome, C. V. (1998) *J. Infect. Dis.* **177,** 683–691
8. Rosenqvist, E., Hoiby, E. A., Wedege, E., Bryn, K., Kolberg, J., Klem, A., Ronnild, E., Bjune, G., and Nokleby, H. (1995) *Infect. Immun.* **63,** 4642–4652
9. Sierra, G. V., Campa, C. H., Varcacel, N. M., Garcia, I. L., Izquierdo, P. L., Sotolongo, P. F., Casanueva, G. V., Rico, C. O., Rodriguez, C. R., and Terry, M. H. (1991) *NIPH Ann.* **14,** 195–207
10. Tappero, J. W., Lagos, R., Ballesteros, A. M., Plikaytis, B., Williams, D., Dykes, J., Gheesling, L. L., Carlone, G. M., Hoiby, E. A., Hoist, J., Nokleby, H., Rosenqvist, E., Sierra, G., Campa, C., Sotolongo, F., Vega, J., Garcia, J., Herrera, P., Poolman, J. T., and Perkins, B. A. (1999) *J. Am. Med. Assoc.* **281,** 1520–1527
11. Vandeputte-Rutten, L., Bos, M. P., Tommassen, J., and Gros, P. (2003) *J. Biol. Chem.* **278,** 24825–24830
12. Prince, S. M., Achtman, M., and Derrick, J. P. (2002) *Proc. Natl. Acad. Sci. U. S. A.* **99,** 3417–3421
13. Masignani, V., Comanducci, M., Giuliani, M. M., Bambini, S., Adu-Bobie, J., Arico, B., Brunelli, B., Pieri, A., Santini, L., Savino, S., Serruto, D., Litt, D., Kroll, S., Welsch, J. A., Granoff, D. M., Rappuoli, R., and Pizza, M. (2003) *J. Exp. Med.* **197,** 789–799
14. Gray-Owen, S. D., and Schyvers, A. B. (1996) *Trends Microbiol.* **4,** 185–191
15. Ala'Aleen, D. A., and Borriello, P. S. (1996) *Vaccine* **14,** 49–53
16. Lissolo, L., Maitre-Wilmotte, G., Dumas, P., Mignon, M., Danve, B., and Quentin-Millet, M. (1995) *Infect. Immun.* **63,** 884–890
17. Webb, D. C., and Cripps, A. W. (1999) *Infect. Immun.* **67,** 2138–2144
18. Myers, L. E., Yang, Y.-P., Du, R.-p., Wang, Q., Harkness, R. E., Schryvers, A. B., Klein, M. H., and Loosmore, S. M. (1998) *Infect. Immun.* **66,** 4183–4192
19. Giuliani, M. M., Santini, L., Brunelli, B., Biolchi, A., Arico, B., Di Marcello, F., Cartocci, E., Comanducci, M., Masignani, V., Lozzi, L., Savino, S., Scarselli, M., Rappuoli, R., and Pizza, M. (2005) *Infect. Immun.* **73,** 1151–1160
20. Welsch, J. A., Rossi, R., Comanducci, M., and Granoff, D. M. (2004) *J. Immunol.* **172,** 5606–5615
21. Bax, A., Vuister, G., Grzesiek, S., Delaglio, F., Wang, A. C., Tschudin, R., and Zhu, G. (1994) *Methods Enzymol.* **239,** 79–105
22. Gagné, S. M., Tsuda, S., Li, M. X., Chandra, M., Smillie, L. B., and Sykes, B. D. (1994) *Protein Sci.* **3,** 1961–1974
23. Ruckert, M., and Otting, G. (2000) *J. Am. Chem. Soc.* **122,** 7793–7797
24. Ottiger, M., Delaglio, F., and Bax, A. (1998) *J. Magn. Reson.* **131,** 373–378
25. Guntert, P. (2000) *Methods Mol. Biol.* **278,** 353–378
26. Banci, L., Bertini, I., Huber, J. G., Luchinat, C., and Rosato, A. (1998) *J. Am. Chem. Soc.*, 12903–12909
27. Pearlman, G., Case, D. A., Caldwell, J. W., Ross, W. R., Cheatham, T. E., DeBolt, S., Ferguson, D. Seibel, G., and Kollman, P. (1995) *Comput. Phys. Commun.* **91,** 1–41
28. Laskowski, R. A., Rullmann, J., MacArthur, M. W., Kaptein, R., and Thornton, J. M. (1996) *J. Biomol. NMR* **8,** 477–486
29. Farrow, N. A., Muhandiram, R., Singer, A. U., Pascal, S. M., Kay, C. M., Gish, G., Shoelson, S. E., Pawson, T., Forman-Kay, J. D., and Kay, L. E. (1994) *Biochemistry* **33,** 5984–6003
30. Grzesiek, S., and Bax, A. (1993) *J. Am. Chem. Soc.* **115,** 12593–12594
31. Peng, J. W., and Wagner, G. (1992) *J. Magn. Reson.* **98,** 308–332
32. Sali, A., and Blundell, T. L. (1993) *J. Mol. Biol.* **234,** 779–815
33. Holm, L., and Sander, C., (1998) *Proteins* **33,** 88–96

34. Pearl, F., Todd, A., Sillitoe, I., Dibley, M., Redfern, O., Lewis, T., Bennett, C., Marsden, R., Grant, A., Lee, D., Akpor, A., Maibaum, M., Harrison, A., Dallman, T., Reeves, G., Diboun, I., Addou, S., Lise, S., Johnston, C., Sillero, A., Thornton, J., and Orengo, C. (2005) *Nucleic Acids Res.* **33,** D247–D251

35. Datta, S., Mori, Y., Takagi, K., Kawaguchi, K., Chen, Z.-W., Okajima, T., Kuroda, S., Ikeda, T., Kano, K., Tanizawa, K., and Mathews, F. S. (2001) *Proc. Natl. Acad. Sci. U. S. A.* **98,** 14268–14273

36. Takagi, K., Yamamoto, K., Kano, K., and Ikeda, T. (2001) *Eur. J. Biochem.* **268,** 470–476

37. Martin, D., Cadieux, N., Hamel, J., and Brodeur, B. R. (1997) *J. Exp. Med.* **185,** 1173–1184

38. Kahler, C. M., Blum, E., Miller, Y. K., Ryan, D., Popovic, T., and Stephens, D. S. (2001) *Infect. Immun.* **69,** 1687–1696

39. Retzer, M. D., Yu, R.-H., and Schryvers, A. B. (1999) *Mol. Microbiol.* **32,** 111–121

40. Renauld-Mongenie, G., Lins, L., Krell, T., Laffly, L., Mignon, M., Dupuy, M., Delrue, R.-M., Guinet-Morlot, F., Brasseur, R., and Lissolo, L. (2004) *J. Bacteriol.* **186,** 850–857

41. Decanniere, K., Transue, T. R., Desmyter, A., Maes, D., Muyldermans, S., and Wyns, L. (2001) *J. Mol. Biol.* **313,** 473–478

42. Sundberg, E. J., and Mariuzza, R. A. (2002) *Adv. Protein Chem.* **61,** 119–160

43. Li, Y., Urrutia, M., Smith-Gill, S. J., and Mariuzza, R. A. (2003) **42,** 11–22

44. Koradi, R., Billeter, M., and Wuthrich, K. (1996) *J. Mol. Graph.* **14,** 29–32

Solution Structure of the Immunodominant Domain of Protective Antigen GNA1870 of *Neisseria meningitidis*

Francesca Cantini, Silvana Savino, Maria Scarselli, Vega Masignani, Mariagrazia Pizza, Giacomo Romagnoli, Erwin Swennen, Daniele Veggi, Lucia Banci and Rino Rappuoli

Access the most updated version of this article at doi: 10.1074/jbc.M508595200

Alerts:
- When this article is cited
- When a correction for this article is posted

Click here to choose from all of JBC's e-mail alerts

Supplemental material:
http://www.jbc.org/content/suppl/2006/01/04/M508595200.DC1

This article cites 38 references, 15 of which can be accessed free at
http://www.jbc.org/content/281/11/7220.full.html#ref-list-1